

Phase Diagrams of the Ternary Systems Mn, Fe, Co, Ni-Si-N*

F. WEITZER AND J. C. SCHUSTER

Institut für Physikalische Chemie, Universität Wien, Währingerstrasse 42, A-1090 Vienna, Austria

Received December 20, 1986

Phase equilibria in the ternary systems Mn, Fe, Co, and Ni-Si-N are investigated and isothermal sections at 900°C (Fe-Si-N, Ni-Si-N), at 1000°C (Mn-Si-N, Co-Si-N) and at 1150°C (Fe-Si-N) are presented. In the system Mn-Si-N, Si₃N₄ coexists with MnSiN₂, Mn₃Si, Mn₅Si₃, MnSi, and MnSi_{2-x}. In the systems Fe, Co, Ni-Si-N, Si₃N₄ coexists with all binary silicides but reacts rapidly with iron above 1120 ± 10°C, and cobalt and nickel above 1170 ± 10°C to form binary silicides and nitrogen gas. © 1987 Academic Press, Inc.

Introduction

Silicon nitride is one of the most attractive advanced ceramic materials of today. Although much is known regarding wetting, metallizing, and joining Si₃N₄ to base metals no rationale of these data in the form of phase diagrams is available. This prompted a systematic investigation of such transition metal-silicon-nitrogen systems and the first set of ternary phase diagrams is presented here.

Literature Review

Liquid manganese wets silicon nitride ($\theta = 74^\circ$) (1) and is reported to react violently with Si₃N₄ at 1270°C under vacuum as well as in inert gas (2). The compounds identified as the reaction products are MnSiN₂, Mn₃Si, and Si₃N₄ (800°C, argon) and Mn₅Si₃ and Si₃N₄ (1200°C, argon), respectively (3). The ternary phase MnSiN₂ is ortho-

rhombic, space group *Pna*2₁, $a = 0.5258$ nm, $b = 0.6511$ nm, and $c = 0.5070$ nm (4). MnSiN₂ was found to form as well by reaction of manganese with silicon under nitrogen (3). The decomposition of MnSiN₂ into MnSi and N₂ gas starts under nitrogen (10⁵ Pa) above 1300°C and under argon above 800°C (3).

Silicon nitride is reported to decompose in contact with iron at temperatures above 700°C (5). This reaction is described to be fast and violent at higher temperatures, especially above the melting point of iron (1, 2, 6). At 1200°C, Si₃N₄ whiskers are observed to be dissolved in an Fe matrix (7). The reaction products found are binary iron silicides and nitrogen gas. A temperature of 1300°C is reported to be necessary to decompose the silicon nitride completely in an alloy Fe + 6 wt% Si₃N₄ in order to obtain an nitride-free alloy (8). The same author observed that at 1150°C the nitrogen evolution is reduced under vacuum compared to a hydrogen atmosphere. Tennenhouse *et al.* (9) investigated the interaction

* Dedicated to Dr. H. Nowotny.

of Si_3N_4 cutting tools with iron and iron-based alloys in air. They conclude that the low melting phase formed during machining is an oxide phase and does not occur in the ternary Fe–Si–N. Joining Si_3N_4 to steel by hot pressing resulted in excellent bonding due to the formation of Fe-silicides in the interlayer. However, due to thermal expansion mismatching, low tensile strength (failure in the Si_3N_4) resulted (10). Iron is often used as an addition in silicon to aid nitridation. The reaction products found are Si_3N_4 and iron silicides (11, 12), which, however, are recognized to be the primary course of strength degradation in hot pressed silicon nitride (13). These results are in agreement with the observation that no bonding takes place and Si_3N_4 is apparently compatible with FeSi (at 1500°C, vacuum, wetting angle $\vartheta = 76^\circ$) and Fe_2Si_5 (at 1450°C, vacuum, wetting angle $\vartheta = 66^\circ$) (14). On the other hand nitriding FeSi₂ leads to the formation of $\text{Si}_3\text{N}_4 + \text{Fe}$ at 1200°C according to Matsumoto *et al.* (15).

Liquid cobalt is reported to decompose Si_3N_4 (1, 6) by the formation of binary silicides and nitrogen gas. The binary silicides CoSi and “Co₃Si” were found to be compatible with Si_3N_4 (14). No bonding to the ceramic was observed. The wetting angles are $\vartheta = 62^\circ$ and $\vartheta < 40^\circ$, respectively. Silicon nitride acts as diffusion barrier between Co and Si in shallow-junction VLSI devices (16).

Liquid nickel is also reported to decompose Si_3N_4 (1, 2, 6) under the formation of binary silicides and nitrogen gas. This reaction was observed to already take place at temperatures above 1000°C (17). These observations are in accord with reports on the degradation of Si_3N_4 whiskers in a nickel matrix in the temperature range between 1000 and 1200°C (7, 18–20). The apparent compatibility of Si_3N_4 with Ni₂Si was concluded from the wetting angle of Ni₂Si on Si_3N_4 ($\vartheta = 108^\circ$, no wetting) (14). Nitriding silicon with the addition of Ni results in

the formation of nickel silicides besides Si_3N_4 (11).

Phase diagram data of the binary silicon–metal and nitrogen–metal systems are taken from literature references: Mn–Si from Moffatt (21); Fe–Si from Schürmann and Hensgen (22); Co–Si from Hansen (23) updated by the work of van den Boomgaard and Carpay (24) as well as Köster *et al.* (25); Ni–Si from Osawa and Okamoto (26), Oya and Suzuki (27), and Ellner *et al.* (28); Mn–N from Zwicker (29), Lihl *et al.* (30), and Kudielka and Grabke (31); Fe–N from Kubaschewski von Goldbeck (32).

No phase diagrams are reported for Co–N and Ni–N. Crystal structure data of the intermediate phases are compiled by Villars and Calvert (33).

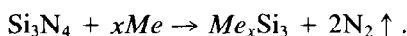
Experimental Procedures

In order to identify all binary silicide phases and to obtain master alloys for further preparation, binary metal–silicon alloys were prepared by arc melting under argon (99.999% pure) from powders or ingots of the constituting elements using the starting materials listed below.¹ Ternary compositions were prepared by mixing powders of these master alloys and binary nitride powders. These ternary mixtures were cold pressed and sintered in evacuated quartz tubes lined with Mo or Ta foil.

X-ray diffraction ($\text{CoK}\alpha_1$ radiation, $\text{CrK}\alpha$ radiation) was performed on all alloys using

¹ Silicon powder, purity m99.9%, from Alpha Div., Ventron Corp., USA; silicon lump, purity m99.9999%, from Alpha Div., Ventron Corp., USA; iron powder, purity 99.5%, impurities (in ppm): Ni 600, C < 600, O < 2000, from Fluka AG, Switzerland; cobalt powder, purity 99.8%, impurities (in ppm): Cu < 50, Pb < 50, Fe < 500, Zn < 50, Ni < 500, Mn < 50; from Fluka AG, Switzerland; nickel powder, purity m99.9%, from Alpha Div., Ventron Corp., USA; silicon nitride (mixture of $\alpha\text{-Si}_3\text{N}_4$ and $\beta\text{-Si}_3\text{N}_4$), powder 58% Si; from Alpha Div., Ventron Corp., USA; manganese nitride (Mn_2N) powder, purity 99.9%, from Alpha Div., Ventron Corp.

Guinier or Debye-Scherrer cameras. In several ternary systems silicon nitride coexists with the transition metal at 1000°C. In order to determine the temperature at which reaction takes place, a large pellet (5–10 g) of the cold compacted powder mixture ($\text{Si}_3\text{N}_4 + 30 \text{ at.}\% \text{ Me}$) was placed in an RF furnace under vacuum and heated slowly. Monitoring with an optical pyrometer the increase in temperature versus the gas pressure (on a logarithmic scale with arbitrary units) permits direct observation of the onset of gas evolution resulting from the reaction



Furthermore the nitrogen gas acts as transporting agents for metallic vapors which are deposited on the quartz window, therefore virtually bringing to an end the optical temperature measurements at the onset of the reaction.

Results and Discussion

The Ternary System Manganese-Silicon-Nitrogen

All phases and crystal structures reported for the binary system Mn-Si (21, 33) could be corroborated and are confirmed. Mn_5Si_2 , found at 700°C, could not be observed at temperatures of 800°C and above. No other discrepancies with the established phase diagram are observed. The lattice parameters found are Mn_6Si ($\text{Mn}_{0.855}\text{Si}_{0.195}$, ϵ -phase), $a = 1.08916 \text{ nm}$, $c = 1.92056 \text{ nm}$; Mn_9Si_2 ($\text{Mn}_{0.815}\text{Si}_{0.185}$, ξ -phase), $a = 1.70195 \text{ nm}$, $b = 2.86750 \text{ nm}$, $c = 0.46675 \text{ nm}$; Mn_3Si $a = 0.57242 \text{ nm}$; Mn_5Si_2 $a = 0.89001 \text{ nm}$, $c = 0.87084 \text{ nm}$, Mn_5Si_3 $a = 0.68988 \text{ nm}$, $c = 0.48096 \text{ nm}$; MnSi $a = 0.45593 \text{ nm}$; and $\text{Mn}_{15}\text{Si}_{26}$ $a = 0.55309 \text{ nm}$, $c = 6.54763 \text{ nm}$. The lattice parameter of $\beta\text{-Mn(s.s.)}$ in an alloy $\text{Mn}_{0.90}\text{Si}_{0.10}$ annealed at 800°C was $a = 0.62869 \text{ nm}$.

In the ternary system the phase MnSiN_2

was formed at 1000°C upon reaction of Si_3N_4 with manganese. MnSiN_2 coexists in the absence of external nitrogen pressure with Si_3N_4 , Mn_3Si , $\beta\text{-Mn(s.s.)}$, and nitrogen gas (Fig. 1). The lattice parameters found are $a = 0.52656 \text{ nm}$, $b = 0.65222 \text{ nm}$, $c = 0.50737 \text{ nm}$ (Si-rich) and $a = 0.52678 \text{ nm}$, $b = 0.65208 \text{ nm}$, $c = 0.50693 \text{ nm}$ (Mn-rich). MnSiN_2 may therefore be considered a line compound having only a very narrow homogeneity range. A three-phase field ($\text{MnSiN}_2 + \text{Mn}_3\text{Si} + \beta\text{-Mn(s.s.)}$) was observed. Hence the stability of Mn_9Si_2 , which was found to exist in the binary Mn-Si system at this temperature, is confined to compositions close to the binary Mn-Si by a tieline between Mn_3Si and $\beta\text{-Mn(s.s.)}$. Si_3N_4 coexists with MnSi_{2-x} , MnSi , Mn_5Si_3 , and Mn_3Si besides MnSiN_2 (Table I). No solubility of nitrogen was observed in any of the manganese silicides. If the external nitrogen pressure is not negligible the formation of $\gamma\text{-Mn(s.s.)}$ modifies the phase equilibria at the Mn-rich corner of the ternary system (Fig. 2). With further increase of the external nitrogen partial pressure, manganese nitrides richer in nitrogen coexist with MnSiN_2 . Thus

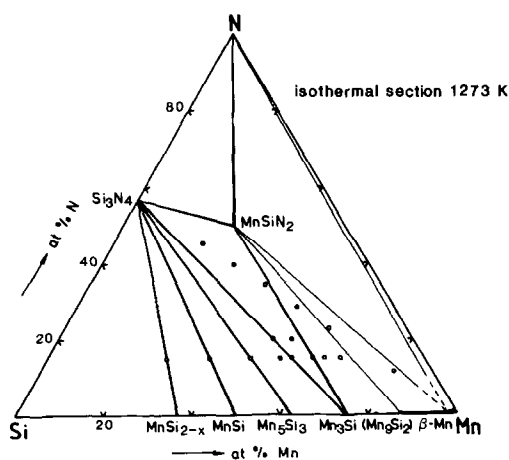


FIG. 1. Isothermal section of the ternary system Mn-Si-N at 1000°C (in the absence of external nitrogen pressure).

TABLE I
SOLID-STATE REACTION PRODUCTS OBSERVED IN THE SYSTEM Mn–Si–N
UPON ANNEALING AT 1000°C, 120 h (EVACUATED QUARTZ TUBES)

$\text{Mn}_{0.366}\text{Si}_{0.634}$ (am) + Si_3N_4 (15 at.% N)	→ Si_3N_4 + MnSi_{2-x}
$\text{Mn}_{0.50}\text{Si}_{0.50}$ (am) + Si_3N_4 (15 at.% N)	→ Si_3N_4 + MnSi + Mn_5Si_3
$\text{Mn}_{0.625}\text{Si}_{0.375}$ (am) + Si_3N_4 (15 at.% N)	→ Si_3N_4 + Mn_5Si_3
$\text{Mn}_{0.714}\text{Si}_{0.286}$ (am) + Si_3N_4 (15 at.% N)	→ Si_3N_4 + Mn_5Si_3 + Mn_3Si
$\text{Mn}_{0.75}\text{Si}_{0.25}$ (am) + Si_3N_4 (15 at.% N)	→ Si_3N_4 + Mn_3Si + MnSiN_2
$\text{Mn}_{0.75}\text{Si}_{0.25}$ (am) + Si_3N_4 (20 at.% N)	→ Si_3N_4 + Mn_3Si + MnSiN_2
$\text{Mn}_{0.818}\text{Si}_{0.182}$ (am) + Si_3N_4 (20 at.% N)	→ Mn_3Si + MnSiN_2
$\text{Mn}_{0.85}\text{Si}_{0.15}$ (am) + Si_3N_4 (15 at.% N)	→ Mn_3Si + MnSiN_2 + $\beta\text{-Mn(s.s.)}$
$\text{Mn}_{0.90}\text{Si}_{0.10}$ (am) + Si_3N_4 (15 at.% N)	→ Mn_3Si + MnSiN_2 + $\beta\text{-Mn(s.s.)}$

Note. am stands for arc-melted.

room temperature X-ray diffraction of alloys annealed at 1273 K under 5×10^4 Pa nitrogen and quenched to liquid nitrogen temperature shows the formation of cubic $\varepsilon\text{-Mn}_4\text{N}$. However, *in situ* high-temperature X-ray diffraction of a specimen having the same nominal composition indicates the existence of a hexagonal phase at 1273 K, confirming Kudielka and co-workers (31).

The Ternary System Iron–Silicon–Nitrogen

All phases and crystal structures reported for the binary Fe–Si system (22, 23) are corroborated and confirmed. According to Kudielka (34) the high-temperature phase Fe_2Si is hexagonal; however, quenching in water was claimed to be insufficient to retain the hexagonal symmetry and a primitive cubic pattern is obtained instead (35). The lattice parameters found are for Fe_2Si : $a = 0.26879$ nm, $c = 0.51281$ nm; FeSi_2 : $a = 0.98789$ nm, $b = 0.78038$ nm, $c = 0.78408$ nm; FeSi : $a = 0.44844$ nm; Fe_5Si_3 : $a = 0.67426$ nm, $c = 0.47146$ nm; $\alpha_2\text{-Fe}_3\text{Si}$: $a = 0.28100$ nm at the Si-rich phase boundary; $\alpha_1\text{-Fe}_3\text{Si}$: $a = 0.5650$ nm (at 75 at.% Fe).

Two isothermal sections have been established in the ternary Fe–Si–N. At 900°C (Fig. 3) Si_3N_4 was found to coexist with all binary silicides stable at this temperature

and $\alpha\text{-Fe}$ (Table II). At 1150°C (Fig. 4) Si_3N_4 is decomposed by pure iron, forming $\alpha\text{-Fe}$ containing 6–8 at.% Si in solid solution. The onset of this decomposition reaction was observed at $1120 \pm 10^\circ\text{C}$. All other binary phases stable 1150°C were found to coexist with Si_3N_4 (Table II). However, as mentioned in the previous section, the phase Fe_2Si could not be observed, probably due to insufficient quenching. Specimens along the tieline Si_3N_4 + Fe_2Si showed the X-ray diffraction patterns of Si_3N_4 , Fe_5Si_3 , and Fe_3Si . It was not possible

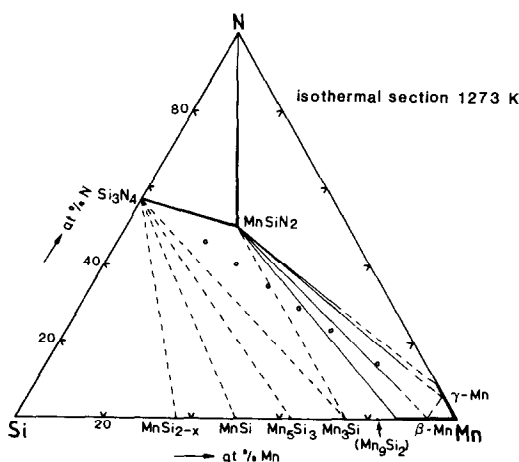


FIG. 2. Isothermal section of the ternary system Mn–Si–N at 1000°C (external nitrogen pressure not negligible).

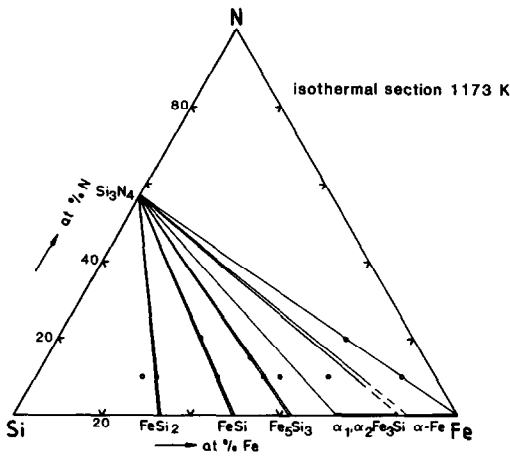


FIG. 3. Isothermal section of the ternary system Fe-Si-N at 900°C (in the absence of external nitrogen pressure).

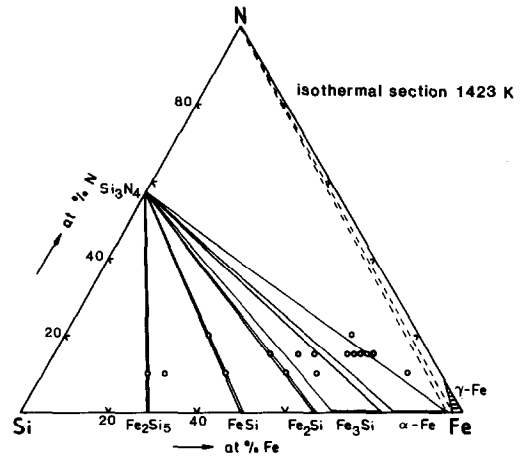


FIG. 4. Isothermal section of the ternary system Fe-Si-N at 1150°C (in the absence of external nitrogen pressure).

to distinguish between α_1 - and α_2 -Fe₃Si due to coincidences of X-ray diffraction lines of Si₃N₄ with the weak lines characteristic for the ordered α_1 -Fe₃Si phase. However, the

smaller lattice parameter of α_2 -Fe₃Si ($a = 0.282$ nm) with respect to the α_1 -Fe₃Si sub-cell ($a = 2 \times a_0 = 2 \times 0.283$ nm) served as an indicator.

TABLE II
SOLID-STATE REACTION PRODUCTS IN THE SYSTEM Fe-Si-N

Upon annealing at 900°C for 340 h (evacuated quartz tube)		
Fe _{0.33} Si _{0.67} + Si ₃ N ₄ (10 at.% N)	→	FeSi ₂ + Si ₃ N ₄
Fe _{0.50} Si _{0.50} + Si ₃ N ₄ (20 at.% N)	→	FeSi + Si ₃ N ₄
Fe _{0.625} Si _{0.375} + Si ₃ N ₄ (15 at.% N)	→	Fe ₅ Si ₃ + Si ₃ N ₄
Fe _{0.67} Si _{0.33} + Si ₃ N ₄ (10 at.% N)	→	Fe ₅ Si ₃ + α_2 -Fe ₃ Si + Si ₃ N ₄
Fe _{0.75} Si _{0.25} + Si ₃ N ₄ (10 at.% N)	→	α_1 -Fe ₃ Si + Si ₃ N ₄
Fe + Si ₃ N ₄ (10 at.% N)	→	α -Fe + Si ₃ N ₄
Fe + Si ₃ N ₄ (20 at.% N)	→	α -Fe + Si ₃ N ₄
Upon annealing at 1150°C for 170 h (evacuated quartz tube)		
Fe _{0.285} Si _{0.715} + Si ₃ N ₄ (10 at.% N)	→	Fe ₂ Si ₅ + FeSi + Si ₃ N ₄
Fe _{0.33} Si _{0.67} + Si ₃ N ₄ (10 at.% N)	→	Fe ₂ Si ₅ + FeSi + Si ₃ N ₄
Fe _{0.50} Si _{0.50} + Si ₃ N ₄ (20 at.% N)	→	FeSi + Si ₃ N ₄
Fe _{0.625} Si _{0.375} + Si ₃ N ₄ (10 at.% N)	→	Fe ₅ Si ₃ + α_2 -Fe ₃ Si ($a = 0.2834$ nm) + Si ₃ N ₄ (insufficient quench)
Fe _{0.67} Si _{0.33} + Si ₃ N ₄ (10 at.% N)	→	α_2 -Fe ₃ Si ($a = 0.2823$ nm) + Si ₃ N ₄
Upon annealing at 1150°C for 60 h (RF-furnace, 10 ⁵ Pa argon)		
Fe _{0.75} Si _{0.25} + Si ₃ N ₄ (15 at.% N)	→	α_1 -Fe ₃ Si ($a = 0.56549$ nm) + Si ₃ N ₄
Fe _{0.90} Si _{0.10} + Si ₃ N ₄ (15 at.% N)	→	α -Fe ($a = 0.28601$ nm) + Si ₃ N ₄

TABLE III
SOLID-STATE REACTION PRODUCTS OBSERVED IN
THE SYSTEM Co-Si-N UPON ANNEALING AT 1000°C,
170 h (EVACUATED QUARTZ TUBES)

$\text{Co}_{0.33}\text{Si}_{0.67} + \text{Si}_3\text{N}_4$ (20 at.% N)	→	$\text{CoSi}_2 + \text{Si}_3\text{N}_4$
$\text{Co}_{0.50}\text{Si}_{0.50} + \text{Si}_3\text{N}_4$ (10 at.% N)	→	$\text{CoSi} + \text{Si}_3\text{N}_4$
$\text{Co}_{0.625}\text{Si}_{0.375} + \text{Si}_3\text{N}_4$ (10 at.% N)	→	$\text{CoSi} + \text{L.T.}-\text{Co}_2\text{Si} + \text{Si}_3\text{N}_4$
$\text{Co}_{0.67}\text{Si}_{0.33} + \text{Si}_3\text{N}_4$ (10 at.% N)	→	$\text{L.T.}-\text{Co}_2\text{Si} + \text{Si}_3\text{N}_4$
$\text{Co} + \text{Si}_3\text{N}_4$ (10 at.% N)	→	$\text{Co}(\alpha + \epsilon) + \text{Si}_3\text{N}_4$

The Ternary System Cobalt-Silicon-Nitrogen

The three intermediate phases reported to exist at 1000°C in the Co-Si system (23-25, 33) are corroborated and confirmed. The lattice parameters found are for CoSi_2 : $a = 0.53526$ nm; CoSi : $a = 0.44449$ nm; $\text{L.T.}-\text{Co}_2\text{Si}$: $a = 0.49073$ nm, $b = 0.37333$ nm, $c = 0.70963$ nm. The high-temperature phases $\text{H.T.}-\text{Co}_2\text{Si}$ and Co_3Si were not observed under the experimental conditions chosen.

At 1000°C Si_3N_4 coexists with cobalt and all binary cobalt silicides stable at this temperature (Table III). The onset of a reaction between Si_3N_4 and Co is found to be at 1170°C from $\log p$ versus temperature data. No ternary phase is observed. No solubility of nitrogen in the binary silicides is detected. An isothermal section at 1000°C is shown in Fig. 5.

The Ternary System Nickel-Silicon-Nitrogen

All the phases and crystal structures reported for the binary system Ni-Si (26-28, 33) are corroborated and confirmed with the exception of the high-temperature modifications of NiSi_2 , Ni_2Si , and Ni_3Si . Attempts to obtain $\text{H.T.}-\text{Ni}_2\text{Si}$ by quenching an alloy from 940 and 1020°C, respectively, into liquid nitrogen did not result in the formation of the desired phase. No specific effort was made to obtain $\text{H.T.}-\text{NiSi}_2$ or $\text{H.T.}-\text{Ni}_3\text{Si}$. The lattice parameters of the silicides found are for $\text{L.T.}-\text{NiSi}_2$: a

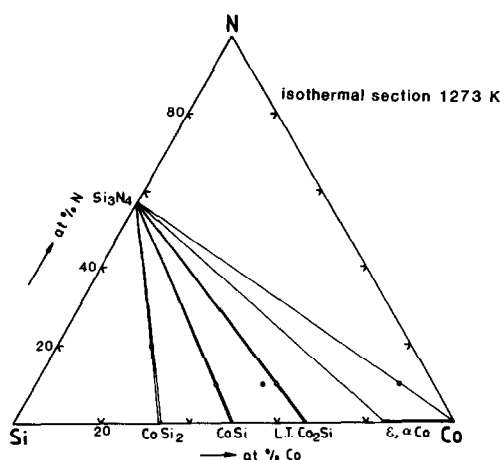


FIG. 5. Isothermal section of the ternary system Co-Si-N at 1000°C (in the absence of external nitrogen pressure).

$= 0.54030$ nm; NiSi : $a = 0.51810$ nm, $b = 0.33365$ nm, $c = 0.56140$ nm; Ni_3Si_2 : $a = 1.22363$ nm, $b = 1.08135$ nm, $c = 0.69213$ nm; $\text{L.T.}-\text{Ni}_2\text{Si}$: $a = 0.50040$ nm, $b = 0.37333$ nm, $c = 0.70715$ nm; $\text{Ni}_{31}\text{Si}_{12}$: $a = 0.66777$ nm, $c = 1.2280$ nm; $\text{Ni}_{25}\text{Si}_9$: $a = 0.67022$ nm, $c = 2.88954$ nm; $\text{L.T.}-\text{Ni}_3\text{Si}$: $a = 0.35098$ nm.

In the ternary system Ni-Si-N Si_3N_4 coexists at 900°C with nickel and all binary nickel silicides stable at this temperature (Table IV). Decomposition of Si_3N_4 by Ni is very fast above 1170°C, but below this temperature Ni and Si_3N_4 seem to coexist. No ternary phase is observed. No solubility of nitrogen in the binary silicides is de-

TABLE IV
SOLID STATE REACTION PRODUCTS IN THE SYSTEM
Ni-Si-N UPON ANNEALING AT 900°C UP TO 340 h
(EVACUATED QUARTZ TUBES)

$\text{Ni}_{0.33}\text{Si}_{0.67} + \text{Si}_3\text{N}_4$ (10 at.% N)	→	$\text{L.T.}-\text{NiSi}_2 + \text{NiSi} + \text{Si}_3\text{N}_4$
$\text{Ni}_{0.50}\text{Si}_{0.50} + \text{Si}_3\text{N}_4$ (10 at.% N)	→	$\text{NiSi} + \text{Si}_3\text{N}_4$
$\text{Ni}_{0.60}\text{Si}_{0.40} + \text{Si}_3\text{N}_4$ (10 at.% N)	→	$\text{Ni}_3\text{Si}_2 + \text{L.T.}-\text{Ni}_2\text{Si} + \text{Si}_3\text{N}_4$
$\text{Ni}_{0.67}\text{Si}_{0.33} + \text{Si}_3\text{N}_4$ (15 at.% N)	→	$\text{L.T.}-\text{Ni}_2\text{Si} + \text{Si}_3\text{N}_4$
$\text{Ni}_{0.715}\text{Si}_{0.285} + \text{Si}_3\text{N}_4$ (15 at.% N)	→	$\text{L.T.}-\text{Ni}_3\text{Si} + \text{Si}_3\text{N}_4$
$\text{Ni}_{0.75}\text{Si}_{0.25} + \text{Si}_3\text{N}_4$ (18 at.% N)	→	$\text{L.T.}-\text{Ni}_3\text{Si} + \text{Si}_3\text{N}_4$
$\text{Ni} + \text{Si}_3\text{N}_4$ (10 at.% N)	→	$\text{Ni} + \text{Si}_3\text{N}_4$

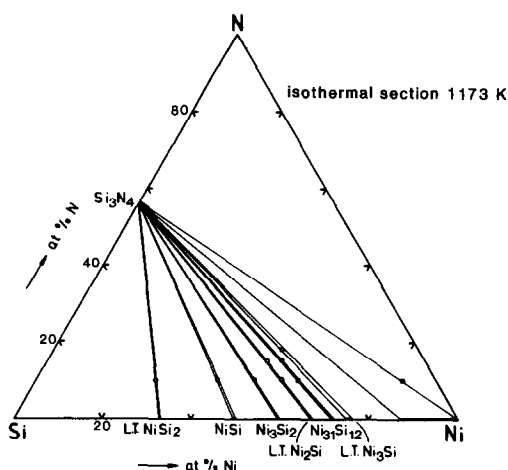


FIG. 6. Isothermal section of the ternary system Ni-Si-N at 900°C (in the absence of external nitrogen pressure).

tected. The isothermal section at 900°C is shown in Fig. 6.

References

1. G. A. YASINSKAYA, *Porosh. Met.* **7**, 53 (1966).
2. H. FELD, E. GUGEL, AND H. G. NITZSCHE, *Werkstoffe Korros.* **20**, 571 (1969).
3. R. POMPE, *Thermochim. Acta* **34**, 245 (1979).
4. R. MARCHAND, M. MAUNAYE, AND J. LANG, *C.R. Acad. Sci. Paris, Ser. C* **272**, 1654 (1971).
5. O. GLEMSE, K. BELTZ, AND P. NAUMANN, *Z. Anorg. Allg. Chem.* **291**, 51 (1957).
6. K. MÜLLER AND H. REBSCH, *Silikattechnik* **17**, 279 (1966).
7. C. A. CALOW AND R. B. BARCLAY, *J. Mater. Sci.* **2**, 404 (1967).
8. D. SIENEL, Kfk-Report 2147 (Kernforschungszentrum Karlsruhe, FRG) p. 53 (1975).
9. G. J. TENNENHOUSE, A. EZIS, AND F. D. RUNKLE, *J. Amer. Ceram. Soc.* **68**, C30 (1985).
10. K. SUGANUMA, T. OKAMOTO, M. KOIZUMI, AND M. SHIMATA, *J. Amer. Ceram. Soc.* **68**, C334 (1985).
11. G. LEIMER AND E. GUGEL, *Z. Metallkd.* **66**, 570 (1975).
12. C. E. BOULDIN, E. A. STERN, M. S. DONLEY, AND T. G. STOEBE, *J. Mater. Sci.* **20**, 1807 (1985).
13. L. HERMANSSON, J. ADLERBORN, AND M. BARSTRÖM, *Rev. Chim. Miner.* **22**, 467 (1985).
14. J. A. CHAMPION, B. J. KEENE, AND S. ALLEN, *J. Mater. Sci.* **8**, 423 (1973).
15. S. MATSUMOTO, Y. KURANARI, K. MAEDA, AND S. INAMOTO, *Japan. Kokai No.* 76.133198 (1976).
16. K. T. HO AND M. A. NICOLET, *Thin Solid Films* **127**, 313 (1985).
17. M. J. BENNETT AND M. R. HOULTON, *J. Mater. Sci.* **14**, 184 (1979).
18. N. J. PARRATT, *Chem. Eng. Prog.* **62**, 61 (1966).
19. E. H. ANDREWS, *J. Mater. Sci.* **1**, 377 (1966).
20. E. H. ANDREWS, W. BONFIELD, C. K. L. DAVIES, AND A. J. MARKHAM, *J. Mater. Sci.* **7**, 1003 (1972).
21. W. G. MOFFATT, "Handbook of Binary Phase Diagrams," General Electric Co., Schenectady, NY (1976).
22. E. SCHÜRSMANN AND W. HENSGEN, *Arch. Eisenhüttenwesen* **51**, 1 (1980).
23. M. HANSEN, "Constitution of Binary Alloys," 2nd ed., p. 504, McGraw Hill, New York (1958).
24. J. VAN DEN BOOMGAARD AND F. M. A. CARPAY, *Acta Metall.* **20**, 473 (1972).
25. W. KÖSTER, H. WARLIMONT, AND T. GÖDEKE, *Z. Metallkd.* **64**, 399 (1973).
26. A. OSAWA AND M. OKAMOTO, *Sci. Rep. Tohoku Univ.* **27**, 326 (1939).
27. T. OYA AND T. SUZUKI, *Z. Metallkd.* **74**, 21 (1983).
28. E. ELLNER, S. HEINRICH, M. K. BHARGAVA, AND K. SCHUBERT, *J. Less-Common Met.* **66**, 163 (1979).
29. W. ZWICKER, *Z. Metallkd.* **42**, 274 (1951).
30. F. LIHL, P. ETTMAYER, AND A. KUTZELNIGG, *Z. Metallkd.* **53**, 715 (1962).
31. H. KUDIELKA AND J. GRABKE, *Z. Metallkd.* **66**, 469 (1979).
32. O. KUBASCHEWSKI VON GOLDBECK, "Iron Phase Diagrams," p. 68, Springer, New York (1982).
33. P. VILLARS AND L. D. CALVERT, "Pearsons Handbook of Crystallographic Data for Intermetallic Phases," American Soc. Met., Metals Park, OH (1985).
34. H. KUDIELKA, *Z. Kristallogr.* **145**, 177 (1977).
35. K. KHALAFF AND K. SCHUBERT, *J. Less-Common Met.* **35**, 341 (1974).